



An Update of Wallace's Zoogeographic Regions of the World

Ben G. Holt *et al.*

Science **339**, 74 (2013);

DOI: 10.1126/science.1228282

This copy is for your personal, non-commercial use only.

If you wish to distribute this article to others, you can order high-quality copies for your colleagues, clients, or customers by [clicking here](#).

Permission to republish or repurpose articles or portions of articles can be obtained by following the guidelines [here](#).

The following resources related to this article are available online at www.sciencemag.org (this information is current as of January 3, 2013):

Updated information and services, including high-resolution figures, can be found in the online version of this article at:

<http://www.sciencemag.org/content/339/6115/74.full.html>

Supporting Online Material can be found at:

<http://www.sciencemag.org/content/suppl/2012/12/19/science.1228282.DC1.html>

This article **cites 678 articles**, 63 of which can be accessed free:

<http://www.sciencemag.org/content/339/6115/74.full.html#ref-list-1>

To examine the temporal profile of ChC production and their correlation to laminar deployment, we injected a single pulse of BrdU into pregnant *Nkx2.1^{CreER};Ai9* females at successive days between E15 and P1 to label mitotic progenitors, each paired with a pulse of tamoxifen at E17 to label NKX2.1⁺ cells (Fig. 3A). We first quantified the fraction of L2 ChCs (identified by morphology) in mPFC that were also BrdU⁺. Although there was ChC production by E15, consistent with a previous study that suggested ventral MGE as a possible source at this time (17), the peak of ChC generation was at E16, when MGE has morphologically disappeared and NKX2.1 expression has appeared at VGZ (Fig. 3, B and C). ChC genesis then diminished but persisted until the end of gestation. This result significantly extends the time course of interneuron generation from NKX2.1 progenitors and suggests that ChCs may be the last cohort, generated at a time when PyN neurogenesis has largely completed. More surprisingly, we found that L5 and L6 ChCs were also BrdU⁺ after E17 induction (Fig. 3, D and E), which indicated that they were generated long after L5 and L6 PyNs, and as late as L2 ChCs. Therefore, the laminar deployment of ChCs does not follow the inside-out sequence, further distinguishing them from MGE-derived interneurons.

NKX2.1 expression during late gestation also included the preoptic area and striatum (6). To prove VGZ as the source of ChCs, we labeled NKX2.1⁺ cells at E16, then transplanted the RFP⁺ VGZ progenitors to the somatosensory cortex of P3 wild-type hosts (Fig. 4, A to B). After 3 weeks, these exogenous progenitors not only differentiated into neurons that spread to the medial frontal areas and settled into appropriate laminae (e.g., L2 and L5) but further matured into quintessential ChCs (Fig. 4, C and D). These results indicate that NKX2.1⁺ progenitors in the late embryonic VGZ are the main source of ChCs. They further demonstrate that the identity of a ChC is determined by its spatial and temporal origin (i.e., lineage and birth time) and, once specified, a cell autonomous program can unfold in ectopic locations, even without proper migration, to direct differentiation.

To examine the role of NKX2.1 in ChC specification, we deleted *Nkx2.1* in VGZ progenitors using a conditional strategy (fig. S8) and transplanted NKX2.1-deficient VGZ cells to the somatosensory cortex of wild-type pups (Fig. 4E). These *Nkx2.1^{KO}* progenitors gave rise to neurons that accumulated in L2 and L5 after 3 weeks (Fig. 4G), a laminar pattern that resembled those of endogenous ChCs. However, *Nkx2.1^{KO}* lineage cells did not differentiate into ChCs, as indicated by the lack of L1 dendrites and almost absence of cartridgelike axon terminals (Fig. 4, F and G). Together with previous studies (6, 7), our results suggest that NKX2.1 may regulate the appropriate temporal competence of progenitors, which likely undergo sequential changes with cell division. They further indicate that NKX2.1 expression in VGZ progenitors is necessary to complete the

specification of a distinct, and probably the last, cohort in this lineage—the ChCs.

A recent study demonstrated that progenitors below the ventral wall of the lateral ventricle (i.e., VGZ) of human infants give rise to a medial migratory stream destined to the ventral mPFC (18). Despite species differences in the developmental timing of corticogenesis, this study and our findings raise the possibility that the NKX2.1⁺ progenitors in VGZ and their extended neurogenesis might have evolved, since rodents, to enrich and diversify cortical interneurons, including ChCs.

Studies in numerous systems (19) have demonstrated that the specification of neuronal identities early in development exerts strong influences in their subsequent positioning, connectivity, and function, but, to what extent this principle applies to the assembly of cortical circuits has been unclear. Here, we discovered that young chandelier cells, once specified through their lineage and birth time in the VGZ, migrate with a stereotyped route and achieve distinct laminar patterns before innervating a subdomain of PyN AIS. Therefore, interneurons with a distinct identity are likely endowed with cell-intrinsic programs that contribute to their subsequent integration into their destined cortical networks. Deficiencies in ChCs have been implicated in brain disorders, including schizophrenia (20). Genetic targeting of ChCs establishes an entry point that integrates studies of fate specification, laminar deployment, connectivity, and network dynamics in the context of cortical circuit assembly and function. This may provide a probe to circuit pathogenesis in models of neuropsychiatric disorders.

References and Notes

1. H. Markram et al., *Nat. Rev. Neurosci.* **5**, 793 (2004).
2. D. M. Gelman, O. Marin, *Eur. J. Neurosci.* **31**, 2136 (2010).

3. G. A. Ascoli et al., *Nat. Rev. Neurosci.* **9**, 557 (2008).
4. J. Szentágothai, M. A. Arbib, *Neurosci. Res. Program Bull.* **12**, 305 (1974).
5. P. Somogyi, *Brain Res.* **136**, 345 (1977).
6. L. Sussel, O. Marin, S. Kimura, J. L. Rubenstein, *Development* **126**, 3359 (1999).
7. S. J. Butt et al., *Neuron* **59**, 722 (2008).
8. H. Taniguchi et al., *Neuron* **71**, 995 (2011).
9. L. Madisen et al., *Nat. Neurosci.* **13**, 133 (2010).
10. J. Szabadics et al., *Science* **311**, 233 (2006).
11. A. Woodruff, Q. Xu, S. A. Anderson, R. Yuste, *Front. Neural Circuits* **3**, 15 (2009).
12. W. Hu et al., *Nat. Neurosci.* **12**, 996 (2009).
13. M. C. Inda, J. DeFelipe, A. Muñoz, *Proc. Natl. Acad. Sci. U.S.A.* **103**, 2920 (2006).
14. J. B. Angevine Jr., R. L. Sidman, *Nature* **192**, 766 (1961).
15. A. Fairén, A. Cobas, M. Fonseca, *J. Comp. Neurol.* **251**, 67 (1986).
16. M. W. Miller, *Brain Res.* **355**, 187 (1985).
17. M. Inan, J. Welagen, S. A. Anderson, *Cereb. Cortex* **22**, 820 (2012).
18. N. Sanai et al., *Nature* **478**, 382 (2011).
19. T. M. Jessell, *Nat. Rev. Genet.* **1**, 20 (2000).
20. D. A. Lewis, *Dev. Neurobiol.* **71**, 118 (2011).

Acknowledgments: We would like to thank G. Miyoshi for technical advice of fate-mapping experiments and helpful discussion. Support by NIH R01 MH094705. H.T. is a Precursor Research for Embryonic Science and Technology investigator supported by Japan Science and Technology Agency and was supported by a Brain and Behavior Research Foundation (NARSAD) Postdoctoral Fellowship. J.L. is in part supported by a Patterson Foundation Postdoctoral Fellowship. Z.J.H. is supported by the Simons Foundation and a NARSAD Distinguished Investigator award.

Supplementary Materials

www.sciencemag.org/cgi/content/full/science.1227622/DC1
Materials and Methods
Figs. S1 to S8
Tables S1 and S2
References (21, 22)
Movie S1

18 July 2012; accepted 1 November 2012
Published online 22 November 2012;
10.1126/science.1227622

An Update of Wallace's Zoogeographic Regions of the World

Ben G. Holt,^{1*} Jean-Philippe Lessard,^{1*†} Michael K. Borregaard,¹ Susanne A. Fritz,^{1,2} Miguel B. Araújo,^{1,3,4} Dimitar Dimitrov,⁵ Pierre-Henri Fabre,⁵ Catherine H. Graham,⁶ Gary R. Graves,^{1,7} Knud A. Jønsson,⁵ David Nogués-Bravo,¹ Zhiheng Wang,¹ Robert J. Whittaker,^{1,8} Jon Fjeldså,⁵ Carsten Rahbek¹

Modern attempts to produce biogeographic maps focus on the distribution of species, and the maps are typically drawn without phylogenetic considerations. Here, we generate a global map of zoogeographic regions by combining data on the distributions and phylogenetic relationships of 21,037 species of amphibians, birds, and mammals. We identify 20 distinct zoogeographic regions, which are grouped into 11 larger realms. We document the lack of support for several regions previously defined based on distributional data and show that spatial turnover in the phylogenetic composition of vertebrate assemblages is higher in the Southern than in the Northern Hemisphere. We further show that the integration of phylogenetic information provides valuable insight on historical relationships among regions, permitting the identification of evolutionarily unique regions of the world.

Biogeographic and bioclimatic regions are the fundamental units of comparison in many broad-scale ecological and evolutionary studies (1, 2) and provide an essential tool

for conservation planning (3, 4). In 1876, Alfred Russel Wallace published the first map of global terrestrial zoogeographic regions (5), which later became the cornerstone of modern biogeography

(3). Using existing knowledge of his time (6), mostly on the distributions and taxonomic relationships of broadly defined vertebrate families, Wallace divided the world into six terrestrial zoogeographic units largely delineated by what we now know as the continental plates. Despite relying on limited information and lacking a statistical basis, Wallace's original map is still in use today.

Wallace's original zoogeographic regionalization scheme considered ancestral relationships among species, but subsequent schemes generally used data only on the contemporary distributions of species without explicitly considering phylogenetic relationships (7–9). Phylogenetic trees contain essential information on the evolutionary relationships of species and have become increasingly available in recent decades, permitting the delineation of biogeographic regions as originally envisioned by Wallace. The

opportunity now exists to use phylogenetic information for grouping assemblages of species into biogeographic units on a global scale. In addition to permitting a sound delimitation of biogeographic regions, phylogenetic information allows quantifying phylogenetic affinities among regions (e.g., 10). Newly developed statistical frameworks facilitate the transparent characterization of large biogeographic data sets while minimizing the need for subjective decisions (11).

Here, we delineated the terrestrial zoogeographic realms and regions of the world (12) by integrating data on the global distributions and phylogenetic relationships of the world's amphibians (6110 species), nonpelagic birds (10,074 species), and nonmarine mammals (4853 species), a total of 21,037 vertebrates species [see (13) for details]. Pairwise phylogenetic beta diversity ($p\beta$) metrics were used to quantify change in phylogenetic composition among species assemblages across the globe. Analyses of combined taxa $p\beta$ values identified a total of 20 zoogeographic regions, nested within 11 larger realms, and quantified phylogenetic relatedness among all pairs of realms and regions (Fig. 1, figs. S1 and S2, and tables S1 and S2). We also used $p\beta$ to quantify the uniqueness of regions, with the Australian (mean $p\beta = 0.68$), Madagascan (mean $p\beta = 0.63$), and South American (mean $p\beta = 0.61$) regions being the most phylogenetically distinct assemblages of vertebrates (Fig. 2). These evolutionarily unique regions harbor radiations of species from several clades that are either restricted to a given region or found in only a few regions.

Our combined taxa map (Fig. 1) contrasts with some previously published global zoogeographic maps derived exclusively from data on the distribution of vertebrate species (8, 9, 11). The key discrepancy between our classification

of zoogeographic regions and these previous classifications is the lack of support for previous Palearctic boundaries, which restricted this biogeographic region to the higher latitudes of the Eastern Hemisphere. The regions of central and eastern Siberia are phylogenetically more similar to the arctic parts of the Nearctic region, as traditionally defined, than to other parts of the Palearctic (fig. S2). As a result, our newly defined Palearctic realm extends across the arctic and into the northern part of the Western Hemisphere (Fig. 1 and fig. S1). These results bear similarities with the zoogeographic map of (11) derived from data on the global distribution of mammal families. In addition, our results suggest that the Saharo-Arabian realm is intermediate between the Afrotropical and Sino-Japanese realms [see the nonmetric multidimensional scaling (NMDS) plot in fig. S2]. Finally, we newly define the Panamanian, Sino-Japanese, and Oceanian realms [but see the Oceanian realm of Udvardy in (14) derived from data on plants].

Our classification of vertebrate assemblages into zoogeographic units exhibits some interesting similarities with Wallace's original classification, as well as some important differences (fig. S3). For example, Wallace classified islands east of Borneo and Bali in his Australian region (fig. S3), which is analogous to our Oceanian and Australian realms combined (Fig. 1 and fig. S1). In contrast, we find that at least some of these islands (e.g., Sulawesi) belong to our Oriental realm, which spans Sundaland, Indochina, and India (Fig. 1 and fig. S1). Moreover, our Oceanian realm is separate from the Australian realm and includes New Guinea together with the Pacific Islands (14), whereas Wallace lumped these two biogeographic units into the Australian region. Wallace further argued that the Makassar

¹Center for Macroecology, Evolution, and Climate, Department of Biology, University of Copenhagen, 2100 Copenhagen Ø, Denmark. ²Biodiversity and Climate Research Centre (BiK-F) and Senckenberg Gesellschaft für Naturforschung, Senckenberganlage 25, 60325 Frankfurt, Germany. ³Department of Biogeography and Global Change, National Museum of Natural Sciences, Consejo Superior de Investigaciones Científicas, Calle de José Gutiérrez Abascal, 2, 28006 Madrid, Spain. ⁴Centro de Investigação em Biodiversidade e Recursos Genéticos, Universidade de Évora, Largo dos Colegiais, 7000 Évora, Portugal. ⁵Center for Macroecology, Evolution, and Climate, Natural History Museum of Denmark, University of Copenhagen, 2100 Copenhagen Ø, Denmark. ⁶Department of Ecology and Evolution, Stony Brook University, Stony Brook, NY 11794–5245, USA. ⁷Department of Vertebrate Zoology, MRC-116, National Museum of Natural History, Smithsonian Institution, Post Office Box 37012, Washington, DC 20013–7012, USA. ⁸Biodiversity Research Group, School of Geography and the Environment, Oxford University Centre for the Environment, South Parks Road, Oxford OX1 3QY, UK.

*These authors contributed equally to this work.

†To whom correspondence should be addressed. E-mail: jplussard@bio.ku.dk



Fig. 1. Map of the terrestrial zoogeographic realms and regions of the world. Zoogeographic realms and regions are the product of analytical clustering of phylogenetic turnover of assemblages of species, including 21,037 species of amphibians, nonpelagic birds, and nonmarine mammals worldwide. Dashed lines delineate the 20 zoogeographic regions identified in this study. Thick

lines group these regions into 11 broad-scale realms, which are named. Color differences depict the amount of phylogenetic turnover among realms. (For more details on relationships among realms, see the dendrogram and NMDS plot in fig. S1.) Dotted regions have no species records, and Antarctica is not included in the analyses.

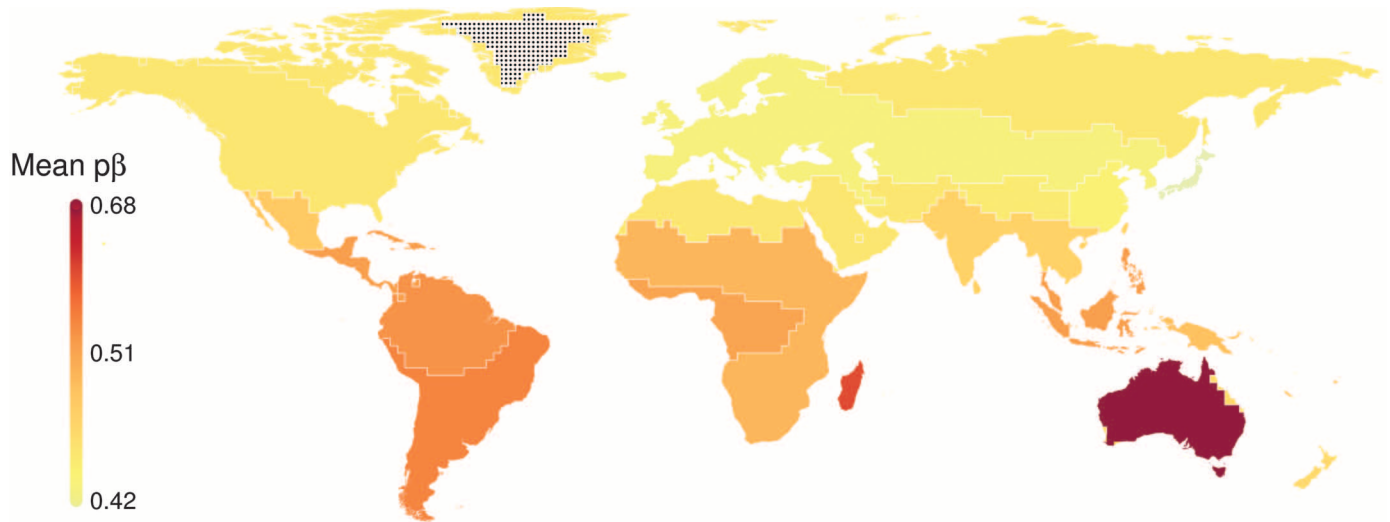


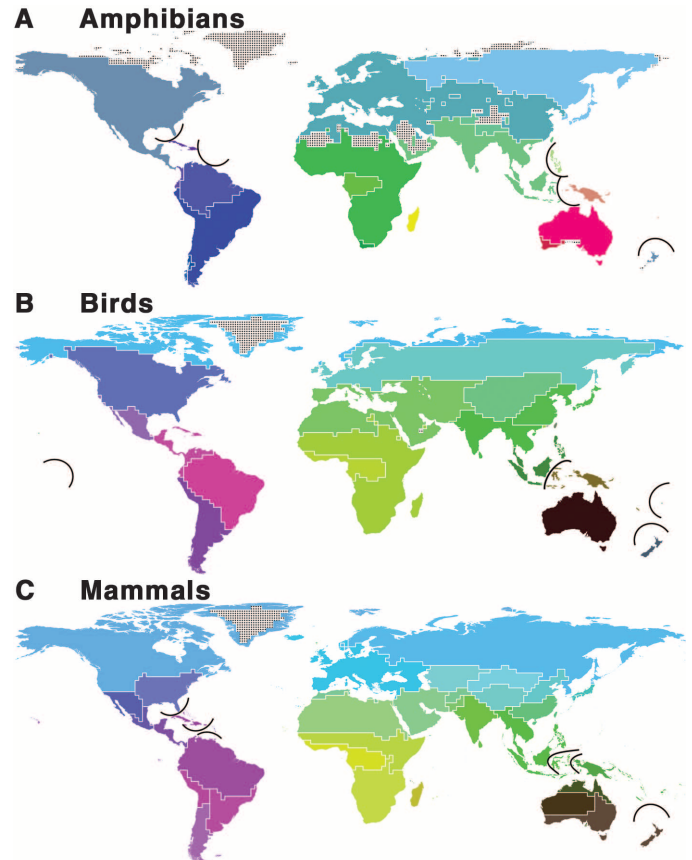
Fig. 2. Map of evolutionary uniqueness for terrestrial zoogeographic regions of the world based on data for 21,037 species of vertebrates. Evolutionary uniqueness is calculated as the mean of pairwise $p\beta$ values between the focal region and all other regions. Colors indicate the degree

to which each region differs from all other regions based on mean pairwise $p\beta$. Regions colored in dark red are the most evolutionarily unique. Dotted regions have no species records, and Antarctica is not included in the analyses.

Strait between Borneo and Sulawesi, now known as “Wallace’s Line” (15), was a major barrier to dispersal that greatly inhibited exchanges between the Australian and Asian land masses. Much debate subsequently arose regarding the precise location of the principal faunal divide between Wallace’s Oriental and Australian realms (15) (see fig. S3 for an illustration of Wallace’s original line). Our combined taxa analyses lend the strongest support to the hypothesis of Weber (16), who positioned this boundary east of Sulawesi, corresponding to the zoogeographic boundary separating our Oriental and Oceanian realms (Fig. 1 and fig. S1). However, our taxon-specific geographic delineation for birds is more consistent with Wallace’s line than Weber’s line (Fig. 3A and figs. S3 and S4A).

The delineation of and relationships among our zoogeographic regions differ among taxa (Fig. 3 and fig. S4), and we find more regions for mammals ($n = 34$ regions) than for amphibians or birds (both $n = 19$ regions). A comparison of $p\beta$ matrices across the three vertebrate taxa reveals that amphibian assemblages located in the northeastern Arctico-Siberian, southern African, and Madagascan regions are more phylogenetically distinct than those of birds or mammals for the same regions (fig. S5). Moreover, the Australian region harbors more phylogenetically distinct assemblages of amphibians and mammals relative to birds (fig. S5). Using a partial Mantel test [see (13) for details on this analysis], which accounts for geographic distances among species assemblages (17), we find that global $p\beta$ values for birds and mammals are more strongly correlated ($r = 0.68$, $P < 0.001$) than for amphibians and birds ($r = 0.39$, $P < 0.001$) or amphibians and mammals ($r = 0.43$, $P < 0.001$). These results might partly reflect a major episode of diversification early in the evolutionary history of amphibians (18). Alternatively, differences in

Fig. 3. Maps of terrestrial zoogeographic regions of the world based on data for (A) amphibians (6110 species), (B) birds (10,074 species), and (C) nonmarine mammals (4853 species). Color differences depict the relative amount of phylogenetic turnover among regions within each taxonomic clade. (For more details on relationships among regions, see the dendrogram and NMDS plots in fig. S4, A to C.) Dotted regions have no species records, and Antarctica is not included in the analyses.



spatial patterns of phylogenetic turnover among vertebrate classes might result from lower dispersal ability (19) and greater sensitivity of amphibians to environmental conditions (20). Interestingly, previous comparative studies documented similar incongruence in the diversity and distribution of amphibians relative to that of birds and mammals (21, 22).

The contrast between our zoogeographic regions with regions based only on distributional data (Fig. 4) demonstrates the consequences of incorporating phylogenetic information in the delineation of zoogeographic units. Relative to expectations based on turnover of species, spatial turnover in the phylogenetic composition of assemblages of species is generally low in the

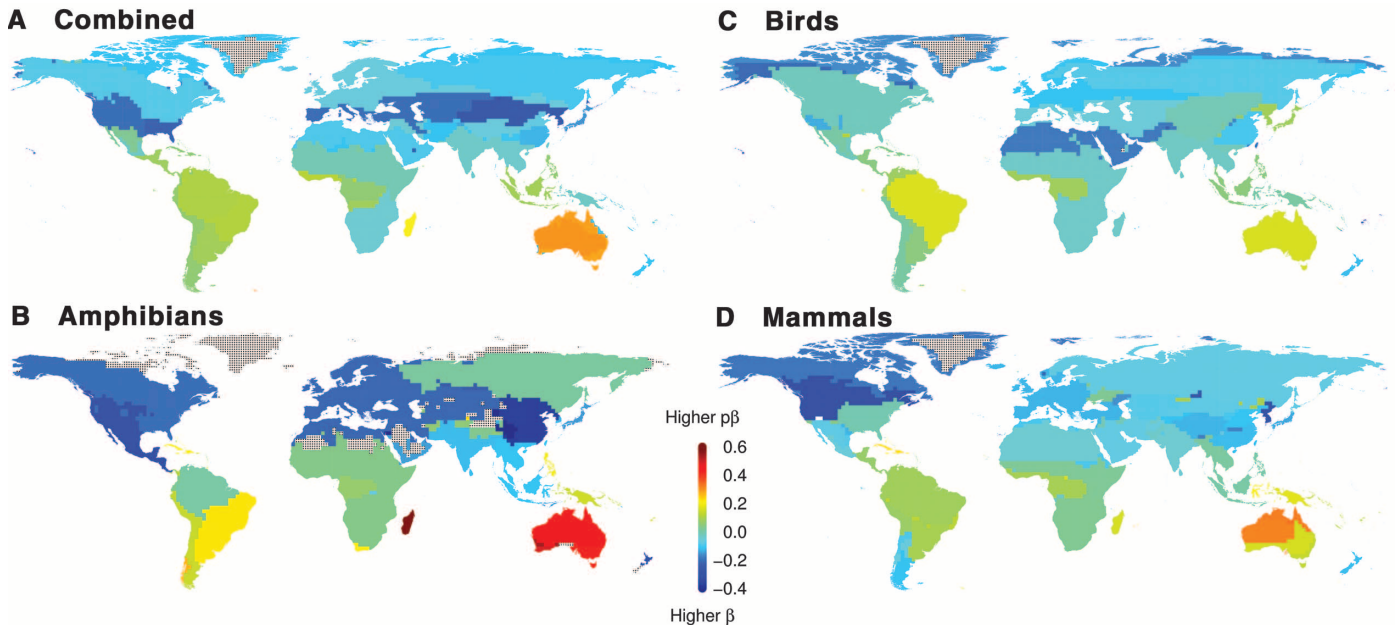


Fig. 4. Combined (A) and taxon-specific (B to D) maps illustrating the degree of phylogenetic turnover relative to the turnover of species observed among zoogeographic regions based on data for species of (A) amphibians, (B) birds, and (C) nonmarine mammals. The color scale depicts the degree to which faunal turnover between the regional assignment of the focal grid cell

and the regional assignment of all other grid cells results from differences in $p\beta$ relative to beta diversity. Red colors indicate regions with a high degree of phylogenetic differentiation relative to compositional differentiation, whereas blue colors indicate the opposite. Dotted regions have no species' records, and Antarctica is not included in the analyses.

Northern Hemisphere, whereas the opposite is true in the Southern Hemisphere (Fig. 4A). In particular, amphibians exhibit low spatial turnover in phylogenetic composition relative to their turnover in the composition of species between the North American and Eurasian regions (Fig. 4B; also compare fig. S4A with fig. S6A). Higher phylogenetic uniqueness in the Southern than in the Northern Hemisphere is consistent with long-term isolation having left a pervasive signature on species assemblages, where oceanic barriers have limited dispersal between continents (23, 24). In the Northern Hemisphere, the newly defined boundaries of the Palearctic realm might reflect the continuous presence of nonglaciated tundra in eastern Siberia and Beringia (25), whereas the subtle differences in the phylogenetic composition of assemblages over the Northern Hemisphere as a whole might be a consequence of a high degree of connectivity and range dynamics. Low rates of extinctions resulting from greater climatic stability in the Southern Hemisphere could also have contributed to this pattern by allowing species that belong to ancient clades to persist through time (26, 27).

Our maps of zoogeographic realms and regions provide a broad overview of the distribution of the world's amphibians, birds, and nonmarine mammals, allowing the identification of geographic areas harboring distinct evolutionary histories [see (28) for links to downloadable maps of zoogeographic realms and regions for projection in GIS (geographic information systems) mapping software and Google Earth]. These maps reflect major advances made in recent dec-

ades regarding our knowledge of the distribution and phylogeny of vertebrates and can be used to elucidate the forces and historical events responsible for the formation of the biogeographic realms and regions we recognize today. Our delineation of the zoogeographic realms and regions of the world, and especially that of the realms, appears robust to the type and quality of distributional and phylogenetic data used [see (13) for details]. Inclusion of additional phylogenetic information on branch length or improved resolution of the phylogenetic trees has the potential to facilitate a finer delineation of regions within our realms. The inclusion of data (when they become available) on reptiles, invertebrates, and/or plants may also affect the boundaries of our realms and regions and the relationships among them. Nevertheless, the maps presented here delineate robust zoogeographic units for vertebrates that can be scaled within specific continents and/or taxonomic clades. Due to these qualities, our analytical approach and zoogeographic maps provide a baseline for a wide variety of comparative ecological, biogeographic, evolutionary, and conservation-based studies (3, 22, 29).

References and Notes

1. M. D. Crisp *et al.*, *Nature* **458**, 754 (2009).
2. S. R. Loarie *et al.*, *Nature* **462**, 1052 (2009).
3. R. J. Ladle, R. J. Whittaker, *Conservation Biogeography* (Wiley-Blackwell, Chichester, UK, 2011).
4. M. V. Lomolino, B. R. Riddle, R. J. Whittaker, J. H. Brown, *Biogeography* (Sinauer Associates, Sunderland, MA, ed. 4, 2010).
5. A. R. Wallace, *The Geographical Distribution of Animals* (Cambridge Univ. Press, Cambridge, 1876).
6. P. L. Sclater, *J. Proc. Linn. Soc. Lond.* **2**, 130 (1858).
7. D. M. Olson *et al.*, *Bioscience* **51**, 933 (2001).
8. Ş. Procheş, S. Ramdhani, *Bioscience* **62**, 260 (2012).
9. C. H. Smith, *J. Biogeogr.* **10**, 455 (1983).
10. C. H. Graham, P. V. A. Fine, *Ecol. Lett.* **11**, 1265 (2008).
11. H. Kreft, W. Jetz, *J. Biogeogr.* **37**, 2029 (2010).
12. A. R. Wallace and his contemporary W. L. Sclater used the terms "region" to denote six main zoogeographical units at a global scale and "subregion" to denote finer scale subdivisions. Wallace's and Sclater's regions and subregions are roughly equivalent to the realms and regions proposed here. The work of Sclater was published in *The Geographical Journal* (1894–1897).
13. Materials and methods are available as supplementary materials on Science Online.
14. M. D. F. Udvardy, *A Classification of the Biogeographic Provinces of the World*, Occasional Paper no. 18 (International Union for Conservation of Nature, Morges, Switzerland, 1975).
15. E. Mayr, *Q. Rev. Biol.* **19**, 1 (1944).
16. M. Weber, *Der Indo-Australische Archipel und die Geschichte Seiner Tierwelt* (Gustav Fischer Verlag, Jena, Germany, 1902).
17. N. Mantel, *Cancer Res.* **27**, 209 (1967).
18. K. Roelants *et al.*, *Proc. Natl. Acad. Sci. U.S.A.* **104**, 887 (2007).
19. M. Munguía, C. Rahbek, T. F. Rangel, J. A. F. Diniz-Filho, M. B. Araújo, *PLoS ONE* **7**, e34420 (2012).
20. L. B. Buckley, W. Jetz, *Proc. Natl. Acad. Sci. U.S.A.* **105**, 17836 (2008).
21. S. A. Fritz, C. Rahbek, *J. Biogeogr.* **39**, 1373 (2012).
22. R. Grenyer *et al.*, *Nature* **444**, 93 (2006).
23. J. Cracraft, *Proc. Biol. Sci.* **268**, 459 (2001).
24. P. Upchurch, *Trends Ecol. Evol.* **23**, 229 (2008).
25. J. R. M. Allen *et al.*, *Quat. Sci. Rev.* **29**, 2604 (2010).
26. J. Fjeldså, E. Lambin, B. Mertens, *Ecography* **22**, 63 (1999).
27. B. Sandel *et al.*, *Science* **334**, 660 (2011).
28. Downloadable maps of zoogeographic realms and regions for visualization in GIS and Google Earth can be found at <http://macroecology.ku.dk/resources/wallace>.
29. K. A. Wilson, M. F. McBride, M. Bode, H. P. Possingham, *Nature* **440**, 337 (2006).

Acknowledgments: We thank the Danish National Research Foundation for its support of the Center for Macroecology,

Evolution, and Climate. B.G.H. also thanks the Marie Curie Actions under the Seventh Framework Programme (PIEF-GA-2009-252888). M.B.A. also thanks the Spanish Research Council (CSIC) for support, and S.A.F. thanks the Landes-Offensive zur Entwicklung Wissenschaftlich-Ökonomischer Exzellenz program of Hesse's Ministry of Higher Education, Research, and the Arts. We thank L. Hansen for help with data and reference

compilations. We thank the International Union for Conservation of Nature and Natural Resources for making the amphibian and mammal range data available. Data are archived at <http://macroecology.ku.dk/resources/wallace>.

Supplementary Materials

www.sciencemag.org/cgi/content/full/339/6115/74/DC1
Materials and Methods

Figs. S1 to S11
Tables S1 to S5
Appendices S1 and S2
References (30–729)

1 August 2012; accepted 15 November 2012
10.1126/science.1228282

Crocodile Head Scales Are Not Developmental Units But Emerge from Physical Cracking

Michel C. Milinkovitch,^{1*} Liana Manukyan,¹ Adrien Debray,¹ Nicolas Di-Poi,¹ Samuel Martin,² Daljit Singh,³ Dominique Lambert,⁴ Matthias Zwicker³

Various lineages of amniotes display keratinized skin appendages (feathers, hairs, and scales) that differentiate in the embryo from genetically controlled developmental units whose spatial organization is patterned by reaction-diffusion mechanisms (RDMs). We show that, contrary to skin appendages in other amniotes (as well as body scales in crocodiles), face and jaws scales of crocodiles are random polygonal domains of highly keratinized skin, rather than genetically controlled elements, and emerge from a physical self-organizing stochastic process distinct from RDMs: cracking of the developing skin in a stress field. We suggest that the rapid growth of the crocodile embryonic facial and jaw skeleton, combined with the development of a very keratinized skin, generates the mechanical stress that causes cracking.

Amniotes exhibit a keratinized epidermis preventing water loss and skin appendages that play major roles in thermoregulation, photoprotection, camouflage, behavioral display, and defense against predators. Whereas mammals and birds evolved hairs and feathers, respectively, reptiles developed various types of scales. Although their developmental processes

share some signaling pathways, it is unclear whether mammalian hairs, avian feathers and feet scales, and reptilian scales are homologous or if some of them evolved convergently (*1*). In birds and mammals, a reaction-diffusion mechanism (RDM) (*2*) generates a spatial pattern of placodes that develop and differentiate into follicular organs with a dermal papilla and cycling

growth of an elongated keratinized epidermal structure (hairs or feathers) (*3*). However, scales in reptiles do not form true follicles and might not develop from placodes (*4*). Instead, reptilian scales originate in the embryo from regular dermo-epidermal elevations (*1*). Whereas the regular spatial organization of scales on the largest portion of the reptilian body is determined by a RDM, additional positional cues are likely involved in the development of the scale plates present on the head of many snakes and lizards. These head scales form a predictable symmetrical pattern (Fig. 1A) and provide mechanical protection.

The face and jaws of crocodilians are covered by polygonal scales (hereafter called “head scales”) that are strictly adjoining and nonoverlapping, but these polygons are irregular and their spatial distribution seems largely random (Fig. 1, B and C). Using high-resolution three-dimensional (3D) geometry and texture reconstructions (*5–7*),

¹Laboratory of Artificial and Natural Evolution (LANE), Department of Genetics and Evolution, University of Geneva, Sciences III, 30, Quai Ernest-Ansermet, 1211 Geneva, Switzerland. ²La Ferme aux Crocodiles, Pierrelatte, France. ³Computer Graphics Group, University of Bern, Switzerland. ⁴Department of Mathematics and Namur Center for Complex Systems, University of Namur, Belgium.

*To whom correspondence should be addressed. E-mail: michel.milinkovitch@unige.ch

Fig. 1. Spatial distribution of head scales. (A) Head scales in most snakes (here, a corn snake) are polygons (two upper panels) with stereotyped spatial distribution (two lower panels): left (yellow) and right (red) scale edges overlap when reflected across the sagittal plane (blue). (B) Polygonal head scales in crocodiles have a largely random spatial distribution without symmetrical correspondence between left and right. (C) Head scales from different individuals have different distributions of scales' sizes and localizations (blue and red edges from top and bottom crocodiles, respectively).

